Journal of Magnetism and Magnetic Materials 497 (2020) 165985

Contents lists available at ScienceDirect

Journal of Magnetism and Magnetic Materials

journal homepage: www.elsevier.com/locate/jmmm

Research articles

Parallel magnetic anisotropy in few layers MoS_2 films

R.G.M. da Fonseca[a], R.F. Albers[b], E.R. Leite[b,c], A.J.A. de Oliveira[a,*]

[a] Physics Department, Federal University of São Carlos, São Carlos, SP, Brazil
[b] Chemistry Department, Federal University of São Carlos, São Carlos, SP, Brazil
[c] Brazilian Nanotechnology National Laboratory, Brazilian Center for Research in Energy and Materials, Campinas, SP, Brazil

ARTICLE INFO

Keywords:
Magnetic anisotropy
Two-dimensional materials
Transition metal dichalcogenides (TMDs)
Van der Waals structures
Molybdenum disulfide

ABSTRACT

Many efforts have been made recently to develop new materials that can be applied in more efficient data storage devices, such as 2D magnetic materials. MoS_2 is the most studied 2D material beyond graphene due to its unique optical, electronic, mechanical and magnetic properties. This paper presents a systematic study of magnetic anisotropy in MoS_2 sheets prepared by liquid exfoliation method. We have applied an extension method in order to obtain ferromagnetic anisotropy by separating paramagnetic contribution from total magnetic anisotropy. MoS_2 thin films exhibit ferromagnetic order on 2D-MoS_2 remaining until room temperature and a magnetization easy plane.

1. Introduction

Data storage devices such as hard disk drive (HDD) [1] mostly employ the physical phenomena of magnetic recording for storing and reading data [2]. It is expected that the growth rate of recording density in a HDD of conventional architecture [3] finds a limit, due to bit instability caused by superparamagnetism [4]. Many efforts have been made in order to design a storage medium that can store data in area densities from 100 to 500 Gbit/in^2 on [5]. Currently, the recording media architecture consists of stacked thin films with typical thicknesses of 11–16 nm composed by magnetic oxides, presenting magnetic moments perpendicularly oriented [3] which could be replaced by individual magnetic atoms adsorbed in a two-dimensional material [6–9], to approach the miniaturization limit of the bit for data storage.

A major breakthrough in the development of more efficient data storage media is to use systems with reduced dimensionality aiming materials that exhibit high magnetic anisotropy energy (MAE), to guarantee the thermal energy k_BT does not exceed the activation energy KV (where K is the anisotropy constant per unit volume and V is the volume), hence the random field fluctuations do not interfere in the spatial orientation of magnetic moments, retaining the stored information [10].

After the discovery of graphene, new perspectives emerged on using 2D materials as a substrate for magnetic atoms [11]. An interesting route to obtain other 2D materials is the use of transition metal dichalcogenides (TMDs) since they can be exfoliated, presenting a general formula MX_2 (where M is the metal and X is the chalcogenide). These materials are X-M-X-type in which the atoms are covalently bonded in plane and the layers interact by van der Waals forces [12]. Among the 2D-TMDs, MoS_2 has attracted much attention due to its promising transport and magnetic properties from a honeycomb hexagonal lattice structure and a strong spin-orbit coupling (SOC), appropriate to present a high magnetic anisotropy [13,14].

Theoretical works have reported magnetic anisotropy of MoS_2 doped with transition metals [15]. The chemical stability and MAE of isolated transition metal atoms (Mn and Fe) adsorbed in MoS_2 monolayers were investigated, based on calculations of first principles and SOC theory showing that transition metal atoms adsorbed in the vacancies of two sulfur atoms are chemically stable and resulted to improve MAE. The easy magnetization axis can be changed from in plane to out of plane by changing the adsorbed atom from Mn to Fe, respectively [16]. Odkhuu et al. calculated that perpendicular MAE is increased to the order of 100 meV per individual ruthenium and osmium atoms adsorbed in a single sulfur atom vacancy in two-dimensional MoS_2 [17]. Furthermore, they stated this giant perpendicular magnetocrystalline anisotropy (PMA) is due to a transition of the spin state involving the hybridization between the molybdenum orbitals and the adsorbed transition metal ones.

In order to develop commercial data storage medium that approaches to the miniaturization limit of the bit, firstly, a synthesis route that enables the deposition of the individual transition metal atoms on the sulfur vacancies must be stablished [16,17] and secondly, there must be a strong bond between the adsorbed transition metal atom and the MoS_2 layer and finally, the material must to present a high MAE. On

* Corresponding author.
E-mail address: adilson@df.ufscar.br (A.J.A. de Oliveira).

https://doi.org/10.1016/j.jmmm.2019.165985
Received 15 November 2018; Received in revised form 14 August 2019; Accepted 12 October 2019
Available online 15 October 2019
0304-8853/

the other hand, it was demonstrated that an anti-site defect (Mo_s) in a MoS_2 layer leads to different values of 1 μ_B, 2 μ_B, and 3 μ_B magnetic moments, which can be replaced by changing Fermi level [18]. A Mo_s in 2D-MoS_2 features a 550 meV MAE with easy axis of magnetization out of plane. Han et al. [19] explored this situation with two approaches: protons irradiation and annealing in H_2 atmosphere, to induce ferromagnetic order in diamagnetic MoS_2 crystals, resulting in an easy axis of magnetization in plane and out of plane, respectively.

Based on in this previous works, we present results of the magnetic behavior of MoS_2 sheets exfoliated in organic solvent [20–23] as a function of applied magnetic field performed in different directions. The dependence of the magnetic behavior of 2D MoS_2 with the directions of applied magnetic field in relation to the basal plane of the sample, measured in different temperature, are explained in terms of the magnetic anisotropy generated by energy balance between the terms of spin-orbit and orbit-crystallographic axes of the states on the zigzag edges. Determining an easy magnetic plane in the basal plane of the MoS_2 sheets.

2. Experimental section

2.1. MoS_2 film preparation

In order to obtain samples with few layers, 1 g of MoS_2 powder (Sigma Aldrich, CAS Number 69860) were added to 100 mL of N-methylpyrrolidine (Sigma Aldrich, CAS Number M79603) and the system was kept under ultrasonication for 6 days (Branson, 1510 ultrasonic bath), with controlled temperature at 25 °C. The material was centrifugated (Eppendorf, Centrifuge 5804) at 11,000 rpm (15557 rcf) for 60 min and 50 µl of the supernatant drops corresponding to 11.5 µg of 2D-MoS_2 were deposited using a micro pipette on the silicon substrate with area and thickness of 3.4×10^6 µm^2 and 546 µm respectively.

2.2. Material characterization

The resulting sample consists of 2D-MoS_2 platelets with the mean basal area of 392 µm^2 and four layers thickness, aligned parallel to the basal plane of the silicon substrate and rotationally disordered.

The morphological analysis was performed by scanning electronic microscopy (SEM), using a FEI microscope (Inspect F-50), beam acceleration between 2 and 5 kV, secondary electrons detector, and transmission electron microscopy (TEM) and electron diffraction, using a Tecnai F-20, operating at 200 kV. To estimate the amount of MoS_2 layers obtained by the exfoliation process, a Micro Raman spectrometer Bruker Senterra was used, with a laser of 532 nm wavelength. And by an atomic force microscope (AFM) EASYSCAN 2 FLEX AFM. The measurements were made in contact mode, where a nitrate tip of Si was used, and the area swept was 1×1 µm^2. Magnetization measurements were performed as a function of applied magnetic field using a Quantum Design SQUID magnetometer, MPMS®3, up to 70 kOe, in the temperature range of 3–300 K, perpendicularly (in relation to the magnetic field) and parallel in angles of 0, 45 and 90° (in the basal plane). For measurements with field parallel the basal plane, the samples were glued on the quartz sample holder purchased by Quantum Design QD part number MPMS 3 (4500-604). For measurements with perpendicular field to basal plane the samples were fixed in a plastic support.

3. Discussion

3.1. Morphological and structural characterization

SEM images of the bulk material, Fig. 1(a), and 2D-MoS_2, Fig. 1(c), showed MoS_2 flakes are deposited with the basal plane parallel to the Si substrate. Comparing Fig. 1(a) and (c) it is noted that the bulk MoS_2 flakes have a lower mean basal area than the 2D-MoS_2 flakes, because the exfoliated sample was prepared with NMP, forming a thin film. The histograms of flakes size distribution of samples, Fig. 1(b), (d) obtained by ultrasonication process, resulted in a narrower flake size distribution, from 30.5 µm^2 ($\sigma = 0.9$) to bulk MoS_2 to 392.8 µm^2 ($\sigma = 0.8$) for 2D-MoS_2 flakes.

TEM images and diffraction pattern, Fig. 2, show a few-layer material. The distance between the atomic planes was 0.307 nm [24,25]. The applied digital method for lattice fringe spacing measurements in HRTEM images, Fig. 2(d), reveals the periodic atom arrangement of the 2D-MoS_2 at a selected location, in which the interplanar spacing was measured to be 0.307 nm according to the periodic pattern in the lattice fringe image, matching up with that of the (0 0 4) facet of 2D-MoS_2 (3.07 Å).

Raman spectrum, Fig. 3(a), exhibited A_{1g} and E^1_{2g} bands as expected for bulk MoS_2 (381.6 and 407.2 cm^{-1}), regarding to the hexagonal lattice structure of the material [26–28], and a shift of these bands was observed for the exfoliated material (379.2 and 404.1 cm^{-1}). The smaller frequency difference between these bands as comparing bulk MoS_2 (25.6 cm^{-1}) and 2D-MoS_2 (24.9 cm^{-1}) indicates the exfoliation process occurred and the exfoliated sample presents on average 4 layers thickness [29,30].

Fig. 3(b) shows AFM image of the surface morphology of the 2D-MoS_2 flakes. Furthermore, in the highlight of Fig. 3(b) show the profile of the exfoliated 2D-MoS_2 flakes swept along the solid line shown in Fig. 3(b) and the following thickness was estimated to be 3.23 nm. This result confirms the estimated of 4 layers performed by the Raman spectroscopy technique.

3.2. Magnetic characterization

Magnetization analysis, Fig. 4, was performed applying a magnetic field up to 70 kOe, in a wide temperature range (3–300 K) to the 2D-MoS_2 flakes. The magnetic field was applied perpendicularly to the basal plane (c direction in the MoS_2 structure) and parallel to the plane of the sample, rotating the angle in 0, 45 and 90°. In all temperatures, the sample exhibited a diamagnetic contribution due to Si substrate, which was subtracted from all curves, Fig. 4. Besides, we observed that a paramagnetic contribution associated to defects is present in the sample [31]. An extension of the anisotropy separation method proposed by Rochette et al. [32] was applied in the magnetization curves in order to subtract the paramagnetic phase contribution of the total anisotropy to obtain the ferromagnetic phase anisotropy. This subtraction was performed using a linear regression in the high field region ($H > 40$ kOe) to calculate the high field magnetic susceptibility (χ_{HF}). The contribution of the ferromagnetic anisotropy is usually saturated in high fields region; therefore, it doesn't influence the linear relation between magnetization and external magnetic field from the paramagnetic phase contribution. And finally, multiplying χ_{HF} by external magnetic field intensity and subtracting the measured magnetization (M).

The magnetization curves measured at 3 K in the different directions of H applied in relation to the basal plane of the sample, Fig. 5(a), are narrow hysteresis cycles [33,34], representative of ferromagnetic systems. Besides, the narrow hysteresis cycles in the different directions of H applied parallel to the basal plane of the sample are isotropic, since the curves present the same S shape, with a small coercive field of 40 Oe (inset). Whereas 2D-MoS_2 flakes magnetic response changes as a function of the field direction, since the curve of the perpendicular measurement is typical of a ferromagnetic material [35,36], with a coercivity of 100 Oe (inset). This anisotropy was demonstrated in a large range of temperature, owing to the fact that the experiments performed up to 300 K resulted in very similar curves when compared to the 3 K measurements, Fig. 5(b).

In the narrow hysteresis cycles in different directions of applied H parallel to the basal plan, Fig. 5(a) and (b) the saturation magnetization was reached in a less intense saturation field (H_s) when compared to the

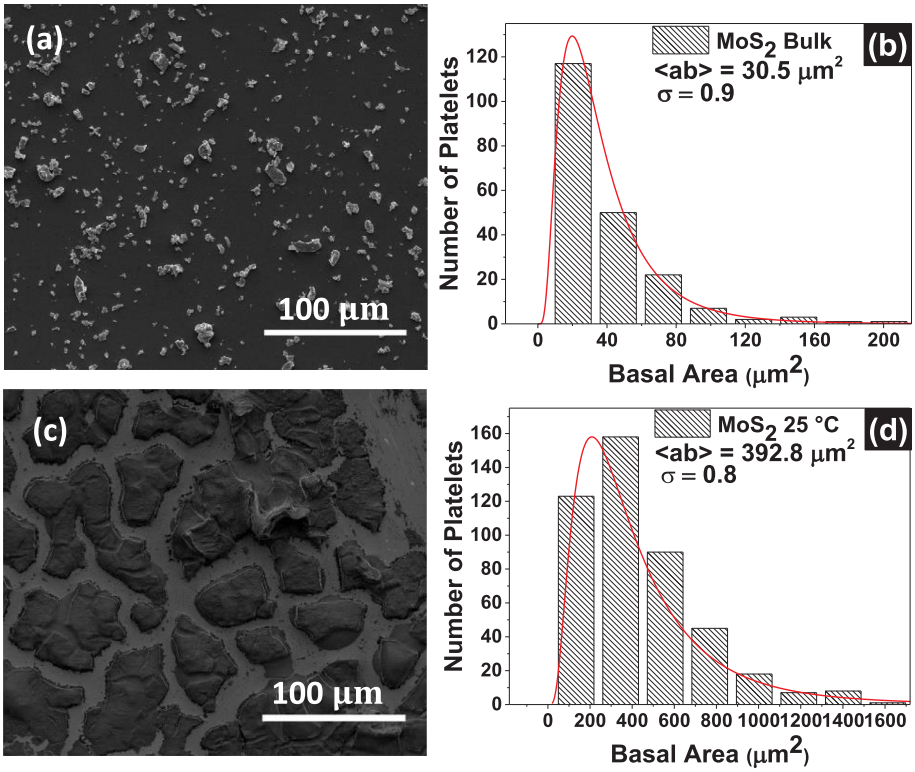

Fig. 1. SEM images of (a) bulk-MoS_2; and (c) 2D-MoS_2 sheets. Histograms and Lognormal function adjust of the basal plane area of (b) bulk MoS_2 flakes and (d) 2D-MoS_2 sheets.

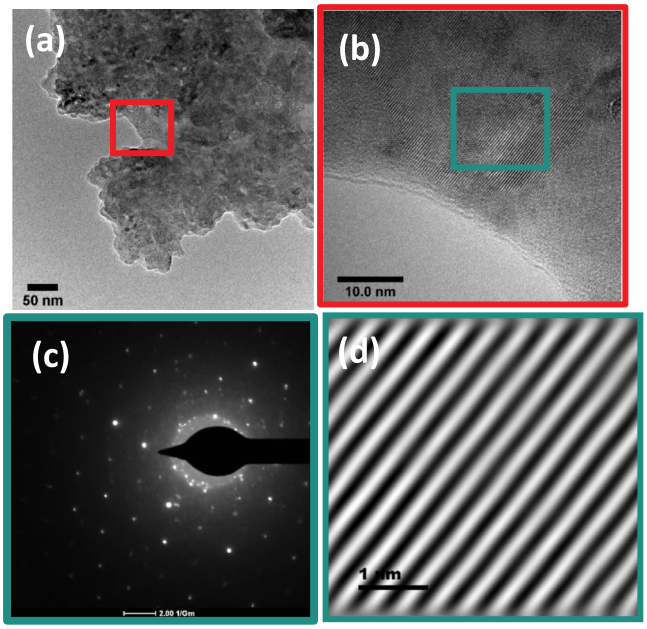

Fig. 2. (a) TEM, (b) HRTEM images, (c) electron diffraction pattern and (d) lattice fringe spacing patterns of 2D-MoS_2.

value obtained when the field was applied in the perpendicular direction. As a consequence, the preferential magnetization direction is parallel to the sample plane, equally easy for the angles 0, 45 and 90°, resulting in an easy magnetization plane. This dependence of the magnetization vector with respect to the directions of H applied in relation to the basal plane of the sample could be attributed to the fact that in 2D systems, with a honeycomb structure, the energy balance between the terms of kinetic, Colombian, spin-orbit and orbit-crystallographic axes energies, that control the ferromagnetic ordering, spin-orbit and the orbit-crystallographic axes interaction of the states on the zigzag edges, is not conventional [37].

The saturation magnetization (M_s) decreases on temperatures up to 30 K, Fig. 5(c), and above 30 K, M_s is no longer dependent on the temperature. Below 30 K, M_s measured in c direction increases, two times higher than the values observed to the other directions. Whereas the values are barely distinguishable for the measurements performed at room temperature (~0.11 emu.g^{-1}) [38]. These induced total magnetic moments are ten times smaller than the value obtained for MoS_2 synthetized films with vertically-oriented edges [39], a hundred times higher than total spontaneous magnetic moment reported as a consequence of decompensated spins in MoS_2 nanosheets edges [40], and in the same order of magnitude of a bulk MoS_2 proton irradiated or annealed in H_2 atmosphere [19] and MoS_2 sheets obtained by chemical vapor deposition (CVD) [36]. This evidence suggests our 4 layers MoS_2 have approximately the same quantity of free spins of proton irradiated MoS_2 and the MoS_2 produced by CVD.

The relation of the coercive field H_c(T) with the temperature in different directions of the applied H in relation to the basal plane of the sample, Fig. 5(d), shows while the H_c(T) measured in the directions of applied H parallel to the plane of the sample presented a well-known decay with temperature, the H_c(T) measured from the magnetization curves measured in the directions of H applied perpendicular to the plane of the sample exhibits an unusual behavior up to 30 K, decreasing to 60 K, and then remaining almost constant up to 300 K. Moreover, the intensity of H_c(T) is higher in the direction of H applied in the perpendicular direction than in H in the parallel direction over the wide temperature range (3–300 K). This anomalous behavior of Hc in relation to the temperature can be well understood when considering that H_c is related to the effective anisotropy constant by the Eq. (1),

$$H_c = \frac{2K_{eff}}{M_s}\left[1 - \left(\frac{25k_B T}{K_{eff} V}\right)^{1/2}\right] \quad (1)$$

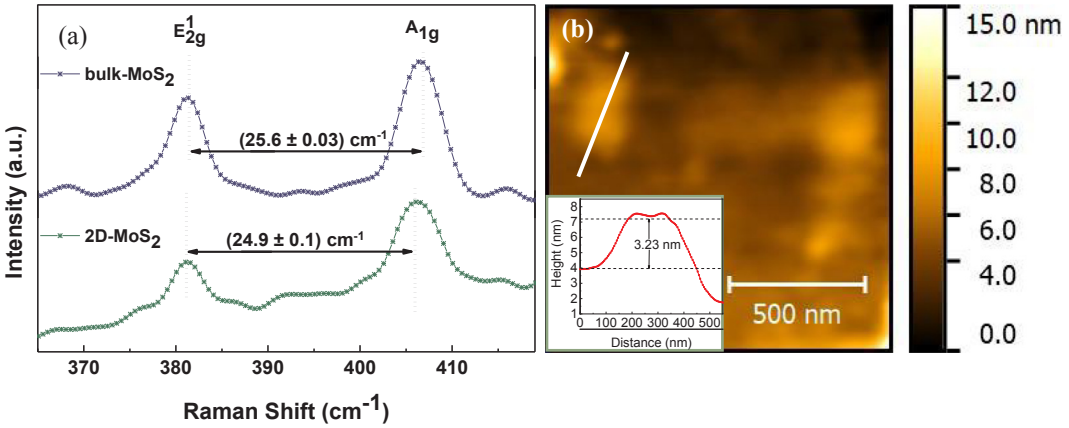

Fig. 3. (a) Raman spectra of bulk-MoS_2 (blue) and 2D-MoS_2 (green). (b) Show the surface morphology of the 2D MoS_2 flakes measured by the AFM technique. In the highlight of (b) show the profile of the exfoliated 2D-MoS_2 flakes swept along the solid line represented in (b). (For interpretation of the references to colour in this figure legend, the reader is referred to the web version of this article.)

where M_s is the saturation magnetization, K_{eff} is the effective anisotropy constant per unit volume and V is the volume. The coercive field is proportional to the effective anisotropy constant and can be calculated from the areas of the magnetization curves obtained for each direction. As the sample presents an easy plane of magnetization, the necessary energy for the applied H, perpendicular to the basal plane of the sample, to rotate the magnetization until reaching the saturation will be higher, due to the boundary condition imposed on the surface of the system in the orbital motion of the decompensated spins of the 2D-MoS_2 contour than when it is applied parallel to the plane. Therefore, the coercive field in the perpendicular direction is higher than in the parallel direction over a wide temperature range (3–300 K). The H_c(T) in perpendicular direction to the basal plane of the sample can be understood in terms of the influence of the temperature on the magnetic anisotropy energy. Initially Hc(T) increases with temperature because the thermal fluctuations induce a smooth displacement of the direction of the magnetization vector relative to the easy plane. Increasing the interaction of the orbital motion with the surface of the system and consequently the energy of the barrier. Thus, thermal fluctuations lead to a greater displacement of the direction of the magnetization vector

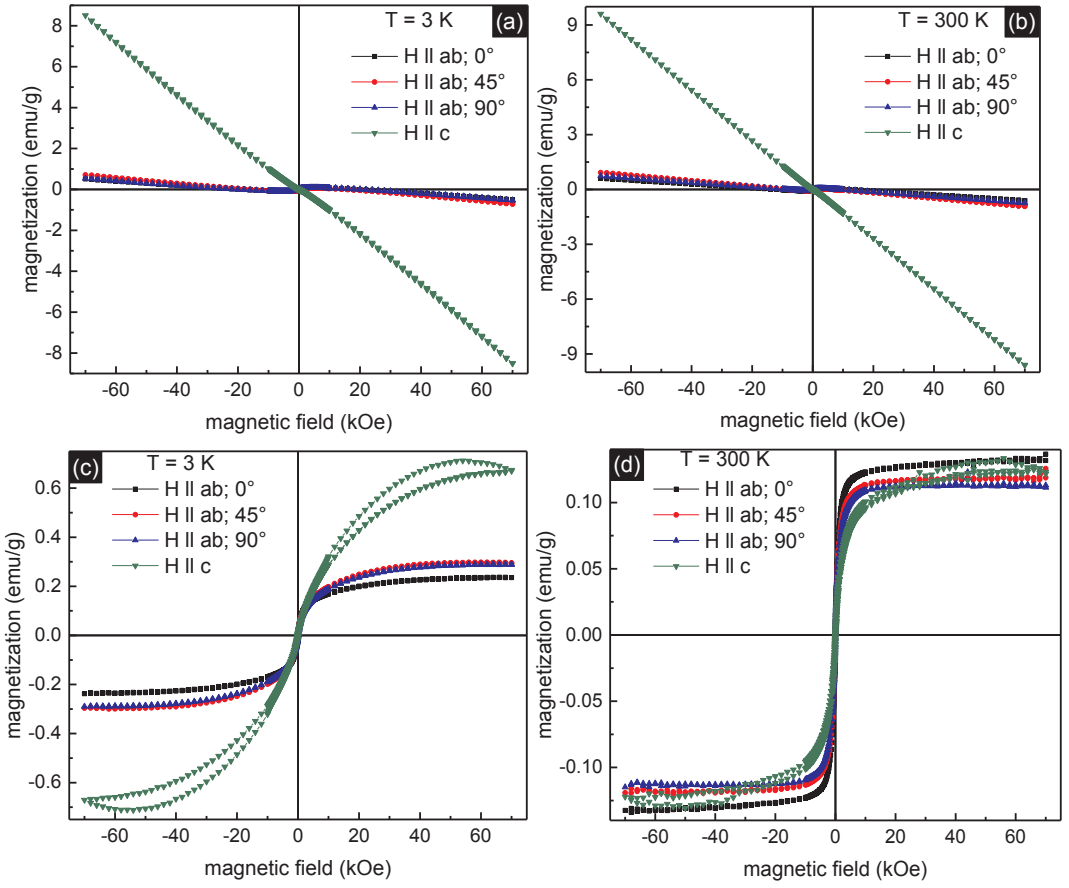

Fig. 4. Magnetization curves data (M vs. H) taken at 3 K (a), (c) and room temperature 300 K (b), (d) when external applied field is perpendicular and parallel in angles of 0, 45 and 90° to the basal planes of the 2D-MoS_2 sheets. (a) and (b) the M vs. H curves of the 2D-MoS_2 sheets was not subtracted the diamagnetism background. After diamagnetism background subtraction, (c) and (d) indicate paramagnetic and ferromagnetic signals of the 2D-MoS_2 sheets have been deducted.

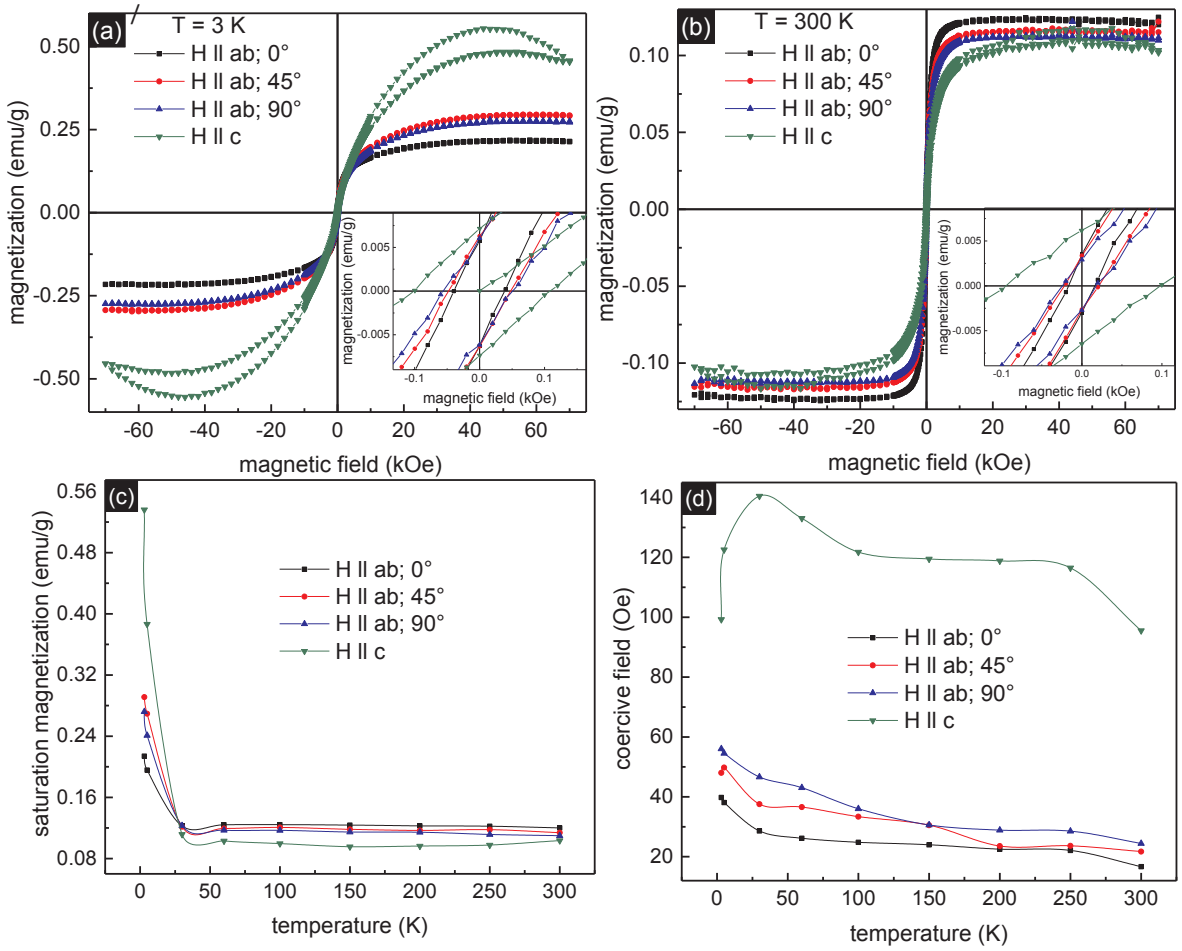

Fig. 5. Magnetization curves at 3 K (a) and 300 K (b) after paramagnetic background subtraction, indicate ferromagnetic signals of the 2D-MoS_2 sheets; saturation magnetization Ms (c) and coercive field Hc (d) vs. temperature curves when external applied field is perpendicular and parallel in angles of 0, 45 and 90° to the basal planes of the 2D-MoS_2 sheets.

until the contour condition imposed by the surface of the system prevents such an increase in the displacement of the direction of the magnetization vector.

4. Conclusion

The findings of this study indicate 2D-MoS_2 sheets prepared by liquid exfoliation method show obvious ferromagnetic order, even at room temperature. Furthermore, the dependence of the coercive field Hc(T) with the temperature measured in different directions of the applied H in relation to the basal plane of the sample was useful in investigations of magnetic anisotropy, showing that there is a preferential magnetization plane parallel to the basal plane. These remarks can lead to a large range of new applications in which magnetic functionalities are fundamental, such as information storage.

Declaration of Competing Interest

The authors declare that they have no conflict of interest.

Acknowledgments

This work was supported by Brazilian Agencies CAPES, CNPq and FAPESP (13/07296-2 and 09/54082-2). The authors are grateful to the microscopy technician Rorivaldo Camargo for TEM images and Professor Valmor Roberto Masteralo from IFSC/USP for XPS measurements.

References

[1] S.N. Piramanayagam, Perpendicular recording media for hard disk drives, J. Appl. Phys. 102 (2007) 011301, , https://doi.org/10.1063/1.2750414.
[2] S. Khizroev, D. Litvinov, Perpendicular magnetic recording: Writing process, J. Appl. Phys. 95 (2004) 4521, https://doi.org/10.1063/1.1695092.
[3] S.J. Lister, T. Thomson, J. Kohlbrecher, K. Takano, V. Venkataramana, S.J. Ray, M.P. Wismayer, M.A. Vries, H. Do, Y. Ikeda, S.L. Lee, Size-dependent reversal of grains in perpendicular magnetic recording media measured by small-angle polarized neutron scattering, Appl. Phys. Lett. 97 (2010) 112503, , https://doi.org/10.1063/1.3486680.
[4] Y. Endo, O. Kitakami, S. Okamoto, Y. Shimada, Determination of first and second magnetic anisotropy constants of magnetic recording media, Appl. Phys. Lett. 77 (2000) 1689, https://doi.org/10.1063/1.1310166.
[5] H.J. Richter, The transition from longitudinal to perpendicular recording, J. Phys. D Appl. Phys. 40 (2007) R149–R177, https://doi.org/10.1088/0022-3727/40/9/R01.
[6] A.A. Khajetoorians, J. Wiebe, Hitting the limit of magnetic anisotropy, Science 344 (2014) 976, https://doi.org/10.1126/science.1254402.
[7] A.A. Khajetoorians, J. Wiebe, B. Chilian, R. Wiesendanger, Realizing all-spin-based logic operations atom by atom, Science 332 (2011) 1062, https://doi.org/10.1126/science.1201725.
[8] S. Loth, S. Baumann, C.P. Lutz, D.M. Eigler, A.J. Heinrich, Bistability in atomic-scale antiferromagnets, Science 335 (2012) 196, https://doi.org/10.1126/science.1214131.
[9] A.A. Khajetoorians, B. Baxevanis, C. Hubner, T. Schlenk, S. Krause, T.O. Wehling, S. Lounis, A. Lichtenstein, D. Pfannkuche, J. Wiebe, R. Wiesendanger, Current-driven spin dynamics of artificially constructed quantum magnets, Science 339 (2013) 55, https://doi.org/10.1126/science.1228519.
[10] O. Hellwing, A. Benger, T. Thomson, E. Dobisz, Z.Z. Bandic, H. Yang, D.S. Kercher, E.E. Fullerton, Separating dipolar broadening from the intrinsic switching field distribution in perpendicular patterned media, Appl. Phys. Lett. 90 (2007) 162516, , https://doi.org/10.1063/1.2730744.
[11] L. Xie, X. Ling, Y. Fang, J. Zhang, Z. Liu, Graphene as a substrate to suppress fluorescence in resonance Raman spectroscopy, J. Am. Chem. Soc. 131 (29) (2009) 9890–9891, https://doi.org/10.1021/ja9037593.

[12] H. Katzke, P. Toledano, W. Depmeier, Phase transitions between polytypes and intralayer superstructures in transition metal dichalcogenides, Phys. Rev. B 69 (2004) 134111, , https://doi.org/10.1103/PhysRevB.69.134111.
[13] Q.H. Wang, K.K. Zadeh, A. Kis, J.N. Coleman, M.S. Strano, Electronics and optoelectronics of two-dimensional transition metal dichalcogenides, Nat. Nanotechnol. 7 (2012) 699–712, https://doi.org/10.1038/nnano.2012.193.
[14] D. Xiao, G.B. Liu, W. Feng, X. Xu, W. Yao, Coupled spin and valley physics in monolayers of MoS_2 and other group-VI dichalcogenides, Phys. Rev. Lett. 108 (2012) 196802, , https://doi.org/10.1103/PhysRevLett. 108.196802.
[15] Z. Chen, J. He, P. Zhou, J. Na, L.Z. Sun, Strain control of the electronic structure, magnetic states, and magnetic anisotropy of Fe doped single-layer MoS_2, Comput. Mater. Sci. 110 (2015) 102–108, https://doi.org/10.1016/j.commatsci.2015.08.010.
[16] D. Odkhuu, Giant perpendicular magnetic anisotropy of an individual atom on two-dimensional transition metal dichalcogenides, Phys. Rev. B 94 (2016) 060403(R), https://doi.org/10.1103/PhysRevB.94.060403.
[17] W.T. Cong, Z. Tang, X.G. Zhao, J.H. Chu, Enhanced magnetic anisotropies of single transition-metal adatoms on a defective MoS2 monolayer, Scientific Rep. 5 (2015) 9361, https://doi.org/10.1038/srep09361.
[18] M.A. Khan, M.N. Leuenberger, Room-temperature superparamagnetism due to giant magnetic anisotropy in Mo_s defected single- layer MoS_2, J. Phys.: Condens. Matter 30 (2018) 155802, , https://doi.org/10.1088/1361-648Xaab113.
[19] S.W. Han, Y. Hwang, S.H. Kim, Y.S. Park, Controlling ferromagnetic easy axis in a layered MoS_2 single crystal, Phys. Rev. Lett. 110 (2013) 247201, , https://doi.org/10.1103/PhysRevLett. 110.247201.
[20] X. Fan, F. Khosravi, V. Rahneshin, B. Panchapakesan, MoS_2 actuators: reversible mechanical responses of MoS_2-polymer nanocomposites to photons, Nanotechnology 26 (2015) 261001, , https://doi.org/10.1088/0957-4484/26/26/261001.
[21] J.T. Han, J.I. Jang, H. Kim, J.Y. Hwang, H.K. Yoo, J.S. Woo, S. Choi, H.Y. Kim, H.J. Jeong, S.Y. Jeong, K.J. Baeg, K. Cho, G.W. Lee, Extremely efficient liquid exfoliation and dispersion of layered materials by unusual acoustic cavitation, Scientific Rep. 4 (2014) 5133, https://doi.org/10.1038/srep05133.
[22] E.D. Grayfer, M.N. Kozlova, V.E. Fedorov, Colloidal 2D nanosheets of MoS_2 and other transition metal dichalcogenides through liquid-phase exfoliation, Adv. Colloid Interface Sci. 245 (2017) 40–61, https://doi.org/10.1016/j.cis.2017.04.014.
[23] J.N. Coleman, Liquid exfoliation of defect-free graphene, Acc. Chem. Res. 46 (1) (2013) 14–22, https://doi.org/10.1021/ar300009f.
[24] X. Guo, Z. Wang, W. Zhu, H. Yang, The novel and facile preparation of multilayer MoS_2 crystals by a chelation-assisted sol–gel method and their electrochemical performance, RSC Adv. 7 (2017) 9009–9014, https://doi.org/10.1039/c6ra25558b.
[25] J. Jeon, S.K. Jang, S.M. Jeon, G. Yoo, Y.H. Jang, J.H. Park, S. Lee, Layer-controlled CVD growth of large-area two-dimensional MoS_2 films, Nanoscale 7 (2015) 1688–1695, https://doi.org/10.1039/c4nr04532g.
[26] G. Deokar, D. Vignaud, R. Arenal, P. Louette, J.F. Colomer, Synthesis and characterization of MoS_2 nanosheets, Nanotechnology 27 (2016) 075604, , https://doi.org/10.1088/0957-4484/27/7/075604.
[27] C. Lee, H. Yan, L.E. Brus, T.F. Heinz, J. Honet, S. Ryu, Anomalous lattice vibrations of single- and few-layer MoS_2, ACS Nano 4 (5) (2010) 2695–2700, https://doi.org/10.1021/nn1003937.
[28] J.L. Verble, T.J. Wieting, Lattice mode degeneracy in mos_2 and other layer compounds, Phys. Rev. Lett. 25 (1970) 362, https://doi.org/10.1103/PhysRevLett. 25.362.
[29] S. Ghatak, A.N. Pal, A. Ghosh, Nature of electronic states in atomically thin MoS_2 field-effect transistors, ACS Nano 5 (10) (2011) 7707–7712, https://doi.org/10.1021/nn202852j.
[30] H. Li, Q. Zhang, C.C.R. Yap, B.K. Tay, T.H.T. Edwin, A. Olivier, D. Baillargeat, From bulk to monolayer MoS_2: evolution of Raman scattering, Adv. Funct. Mater. 22 (2012) 1385–1390, https://doi.org/10.1002/adfm.201102111.
[31] M. Sepioni, R.R. Nair, S. Rablen, J. Narayanan, F. Tuna, R. Winpenny, A.K. Geim, I.V. Grigorieva, Limits on intrinsic magnetism in graphene, Phys. Rev. Lett. 105 (2010) 207205, https://doi.org/10.1103/PhysRevLett.105.207205.
[32] F.M. Hernandez, E.C. Ferre, Separation of paramagnetic and ferrimagnetic anisotropies: a review, J. Geophys. Res. 112 (2007) B03105, https://doi.org/10.1029/2006JB004340.
[33] S. Mathew, K. Gopinadhan, T.K. Chan, X.J. Yu, L. Cao, A. Rusydi, M.B.H. Breese, S. Dhar, Z.X. Shen, T. Venkatesan, T.L. Thong, Magnetism in MoS_2 induced by proton irradiation, Appl. Phys. Lett. 101 (2012) 102103, , https://doi.org/10.1063/1.4750237.
[34] S. Tongay, S.S. Varnoosfaderani, B.R. Appleton, J. Wu, A.F. Hebard, Magnetic properties of MoS_2: existence of ferromagnetism, Appl. Phys. Lett. 101 (2012) 123105, , https://doi.org/10.1063/1.4753797.
[35] R. Zhang, Y. Li, J. Qi, D. Gao, Ferromagnetism in ultrathin MoS_2 nanosheets: from amorphous to crystalline, Nanoscale Res. Lett. 9 (2014) 586, https://doi.org/10.1186/1556-276X-9-586.
[36] Z. Yang, D. Gao, J. Zhang, Q. Xu, S. Shi, K. Tao, D. Xue, Realization of high Curie temperature ferromagnetism in atomically thin MoS_2 and WS_2 nanosheets with uniform and flower-like morphology, Nanoscale 7 (2015) 650–658, https://doi.org/10.1039/c4nr06141a.
[37] J.L. Lado, J.F. Rossier, Magnetic edge anisotropy in graphenelike honeycomb crystals, Phys. Rev. Lett. 113 (2014) 027203, , https://doi.org/10.1103/PhysRevLett. 113.027203.
[38] D. Gao, S. Shi, K. Tao, B. Xia, D. Xue, Tunable ferromagnetic ordering in MoS_2 nanosheets with fluorine adsorption, Nanoscale 7 (2015) 4211–4216, https://doi.org/10.1039/c5nr00409h.
[39] J. Zhang, J.M. Soon, K.P. Loh, J. Yin, J. Ding, M.B. Sullivian, P. Wu, Magnetic molybdenum disulfide nanosheet films, Nano Lett. 7 (8) (2007) 2370–2376, https://doi.org/10.1021/nl071016r.
[40] D. Gao, M. Si, J. Li, J. Zhang, Z. Zhang, Z. Yang, D. Xue, Ferromagnetism in free-standing MoS_2 nanosheets, Nanoscale Res. Lett. 8 (2013) 129, https://doi.org/10.1186/1556-276X-8-129.